

# Designing a Platform for Organ Motion Simulation with Surgical Robotics

Abhishek Jain, Kavit Nilesh Shah, Peter Guglielmino, Rishi Madduri,

Soumya Balijepally, Thejus Jose, Zainab Khan

*Mechanical / Robotics Engineering Department*

*Worcester Polytechnic Institute*

**Abstract**—Complex medical surgeries need expert training and precision before being conducted on a patient. A challenge in many surgeries is the presence of moving organs such as beating hearts and breathing lungs. A precise method to account for motion compensation in surgery would help improve medical procedures. This project aims to design, develop, and test a robotic platform capable of mimicking the motion of human organs that can be used in the workspace of a DaVinci robot in order to train surgeons. The platform is based on the design of a stewart platform and can essentially take any given motion data and produce simulated organ motion. The design phase involved developing a hardware model for the prototype and a software simulation which incorporates the mathematical model, trajectory planning, inverse kinematics, and position-velocity controller. For the initial experimentation of the platform, chest motion data was obtained and processed to generate a desired motion trajectory. Inverse kinematics were performed to extract joint angles for the servo motors of the platform. A full simulation model was developed in Simscape Multibody. Results were used to further tune the performance of the platform and fabricate the hardware prototype model. The proposed platform aims to improve accuracy and mimic chest breathing motion.

## I. INTRODUCTION

### A. Background

Successful surgical performance requires a refined skill set which is developed through hours of practice and exposure. With the numerous new sub-specializations in medical surgery, it can no longer be expected for medical students to gain all necessary skills in a clinical environment [5]. A major challenge in surgical training is providing an ideal practice environment for effective learning without jeopardizing the health of the patient. With surgical simulation, the educational needs of medical students can be met in a safe, non-clinical environment, geared towards the needs of the student rather than the patient. Student performance can be gauged objectively and students can be given room to fail and improve [3]. Hence, simulation of surgery can be more effective for students and safer for patients [5, 3]. Different approaches of model-based and computer-based simulation have been developed over the recent years. Hybrid systems merge both approaches for a more realistic experience [3]. Virtual reality environments are also being developed for a better simulation experience. With the advent of surgical robots, complex surgeries which require extreme precision and mental coordination can be more accurately done with the help of robots. Commonly, the movement of an organ during operation is passively suppressed

or shut down temporarily [7]. However, these methods are not practical for long periods of time [4]. Alternatively, in a robotics system, organ motion compensation can be incorporated in the control loop to operate on beating hearts and respiring lungs. Organ motion is a challenge particularly in cardiac surgery. Due to the rapid and unpredictable movements of the heart, dynamic control approaches are required to cancel out the effect of its motion [4]. Mechanical platforms which simulate the movement of the organ need to be designed to test new control methods in coordination with surgical robots. Lungs, eyes and the oesophagus are some other organs whose unpredictable involuntary movements cannot be eliminated during surgery. Lung surgeries often involve performing biopsies or surgeries to remove fluid build-up in cases of pneumonia or removal of blood from the chest cavity. Some eye surgeries are still performed without lasers and automatic motion compensation. In all these cases, there is a constant risk of injuring the blood vessels or causing prolonged air leak, causing severe problems if not operated with precision. As a result, it is imperative that surgeons be thoroughly trained on a realistic physical simulation of these organs before being allowed to perform surgery.

The work presented in this report develops a platform to address this concern. The platform is based on the popular stewart platform design and uses rotary actuators rather than the more common linear hydraulic/pneumatic actuators in order to achieve more precise control. The goal of this work is to develop a platform that can accurately mimic the motion of a chest during regular breathing.

### B. Literature Review

The past work done on robotic platforms for training in robotic surgery is very limited. The most sophisticated platforms are mostly used for motion compensation experiments in order to test controllers for surgical robot arms with the ability to follow the motion of the organ. These testbeds are usually of three kinds: 1 DOF platforms, live animals or humans.

A number of experiments have been performed using a simple 1 DOF platform to simulate the target motion to be compensated by the robotic manipulator [2, 12]. The work performed in [2] and [12] approximate the motion of the mitral valve of the heart as a 1D motion in order to justify the use of a 1 DOF testbed. However, *in vivo* tests suggest that this motion involves some off-axis components due to the respiration of

the subject. These components of motion are compensated either manually by the surgeon or by momentarily stopping the controlled ventilation to the patient.

The use of live animals or human subjects is also common in the testing of motion compensation devices [7, 8]. While human subjects can legally only be used after the safety of the device has been validated by numerous simulations and tests, the regulations for using live animals are not so stringent. Nonetheless, the use of live animals involves a number of ethical and legal complications, which slows down the experimentation process. Moreover, the degree to which the organs of the live animal mimic the motion of the human organ also depends on a number of factors.

The work of Wilbert, et al. [11] is one of the very few papers that uses a 6-axis robotic arm to simulate the motion of a tumour. A tumour phantom is placed on the end of the arm and its motion paths are defined by time-indexed control points. The large size of the 6-axis robotic arm creates a two-fold problem. First, the testbed will not be able to fit within the workspace of the daVinci robot which is the target surgical robot of the current work. Second, a large size induces high inertia which means that the robot cannot mimic high speed, high frequency motions such as the beating of a heart.

Patel, et al. [6] attempts to develop a universal organ motion simulator to mimic the motion of any organ and overcome some of the problems faced by other platforms. A stewart platform coupled with high precision motors is used in order to make the robot capable of high frequency motions.  $R^2$  values of 0.69, 0.49, and 0.14 for x, y, and z respectively were achieved.

This work attempts to extend the work of [6] and improve accuracy while also making the platform capable of mimicking motion of a moving chest during surgery.

## II. METHODOLOGY

### A. Design

The design of Stewart Platform was motivated by our goal to build a 6 degrees-of-freedom robot platform to simulate the motion of lung during non-invasive surgeries performed by the daVinci surgical robot. The dimensional constraints were taken according to those of the daVinci workspace. The platform is powered by MG-995 which provides a stall torque of 13 kg-cm.

#### 1) Design Factors:

a) *Dimensions of the top surface:* The dimensions of the top surface for the model depends on workspace constraints of the daVinci surgical system. The models dimensions in-turn affect the stability and range of motion of the model.

b) *Geometrical constraints:* The positions of joint mounts on the top end and bottom layer affect the kinematics of the platform in terms of range of motion.

c) *Degrees of freedom:* It is necessary to determine the minimum degrees of freedom needed to achieve the required motion. The DOFs will influence the design of the model by determining the geometry, number of actuators and type of

actuators needed as well as by determining the configurations that are achievable by the platform.

d) *Workspace constraints:* The design of the model will be constrained by the workspace it is intended to work in. These constraints include the dimensions of the base of the platform and the height. The design requires a wide base as well as a wide platform to accommodate larger surgical simulation tools.

e) *Motion constraints:* The type of joints and joint mounts along with the direction of motion are factors which affect the dynamics of the platform.

f) *Actuator parameters:* Parameters like range of motion of the model, frequency range of operation and speed of the actuators, dimensions constraints, stall torque, response time in-turn shape the design parameters.

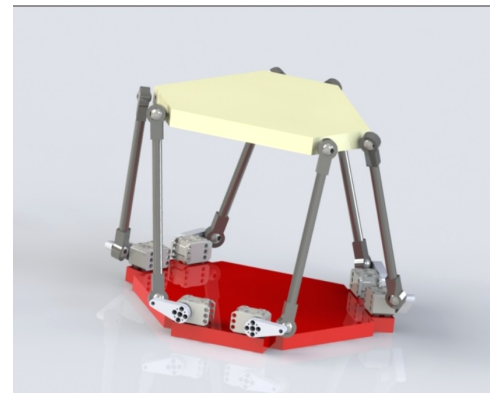


Fig. 1. Stewart Platform (D1)

The platform gets its versatility from Heim joint or Ball and socket joint. The first design of the platform had a simple ball and socket joint between the connecting rod and the arm link.

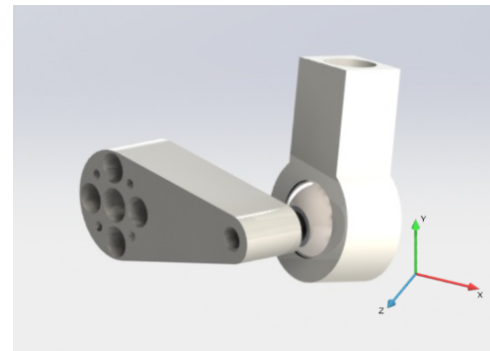


Fig. 2. Heim Joint (D1)

The second design D2 consists of an improved Heim joint as well as a different orientation of the top platform with respect to the base. The new design allows a wider range of motion than what was permitted in D1. The Heim joint of D2 resembles a knuckle joint and has a range of motion of up to 80 degrees in contrast to D1 which allowed only 60 degrees.

The improved design offers more flexibility in terms of Roll, Pitch and Yaw.

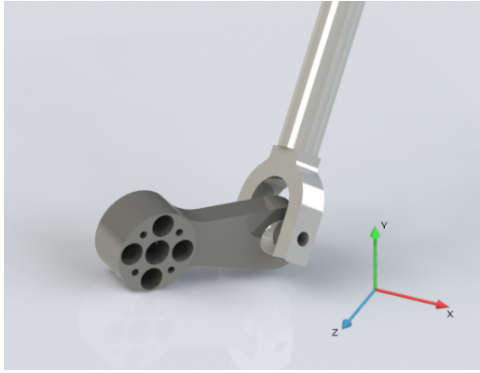


Fig. 3. Heim Joint (D2)

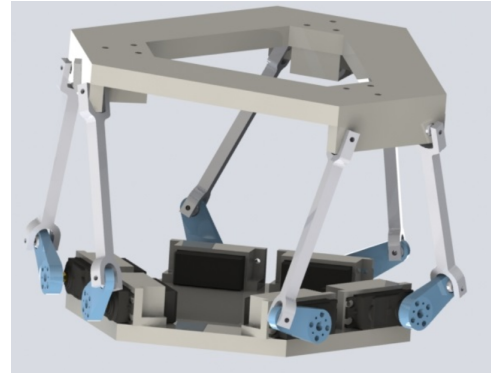


Fig. 6. Stewart Platform (D3)

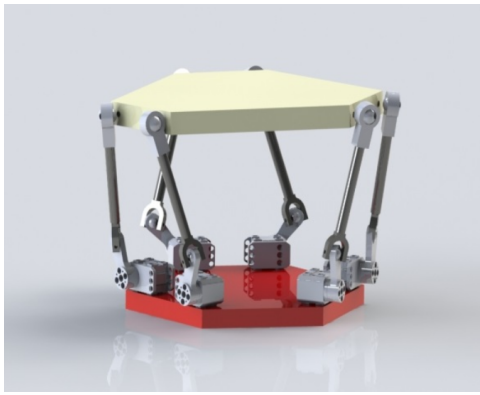


Fig. 4. Stewart Platform (D2)

The final iteration of design of the stewart platform consists of a custom heim joint (D3) with the ball and the crank arm designed as a single component.

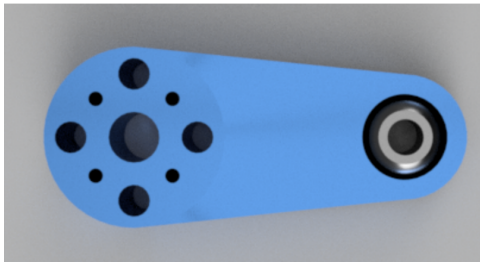


Fig. 5. Heim Joint (D3)

The mounts on the bottom plate were designed to hold the Servos in place during the motion of the stewart platform. The connecting rods were fixed to the top plate with the help of another set of ball joints that provide a more flexible Roll, Pitch and Yaw.

#### B. Data Acquisition

A set of data points for chest breathing motion was collected from a previous study which presented multiple datasets taken by VICON motion capture [9]. The study was performed for human breathing motion under four different types of

Component	Parameter
Lower Base Radius	102mm
Upper Base Radius	118mm
Connecting Rod Length	110mm
Crank Arm	30mm
Effective Side Length of Lower Base	82mm
Effective Side Length of Upper Base	60mm
Height of Platform in Home Position	125mm
Crank Angle at Home Position	30 degrees

TABLE I  
DESIGN PARAMETERS

breathing: free breathing, post exercise breathing, irregular breathing and apnoea manoeuvre of which free breathing was selected for our study. Any other breathing type could also be selected with no bias for one type over the other. Each of the 16 motion trackers record the x, y and z motion of each point w.r.t t.

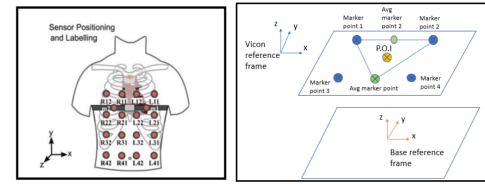


Fig. 7. (a): Shafiq, G. and Veluvolu, K. C. Multimodal chest surface motion data for respiratory and cardiovascular monitoring applications, (b): Data acquisition configuration implemented

For obtaining real-time position and orientation data of the point of interest (P.O.I), only three marker points are needed around the POI forming an equilateral triangle with POI at its centroid. The requirement of three marker points arises as three points define a plane. Since, such a configuration of marker points is not available in the current dataset, four instead of three points are selected around the POI. Motion tracker R11, L12, R21 and L22 as seen in fig 8a are used for this project. As seen in fig 8b, configuration of three marker points is achieved by taking the average of two out of the four marker points (marker points 3 and 4 in this case). Mean of the data of marker points 1, 2 and Average marker point gives the motion data of out POI of interest. Since all motion trackers are calibrated w.r.t Vicon reference frame, a transformation

had to be applied to shift the data of all the points from Vicon reference frame to base reference frame.

To obtain the orientation data of the top platform, rotation matrix is calculated for the top platform wrt base at each time instant. The equation of plane is calculated at each time step and the normalized coefficients of plane equation represent unit normal to the plane which is z-axis of top platform wrt base. Average marker point 2 represents the average of marker points 1 and 2. A normalized vector from POI to average marker point 2 represents the y-axis and cross product of y-axis with z-axis gives the x-axis of top platform wrt base. Once the x, y and z-axes of top platform are obtained with respect to base for each time step, the rotation matrix for the top platform with respect to base is computed using the dot product form of rotation matrix. Thus, the real-time position and orientation data is obtained.

### C. System Modeling and Control

Once the data is processed and translated as xyz points, it is fed into an inverse kinematics model to obtain joint angles for each servo motor. A trajectory planner interpolates the data for each joint angle for smoother motion and gives the target position and velocity with respect to time. The generated trajectory is fed as an input to a PD position controller, developed in Simulink, to minimize error. The controller outputs a force for each joint which is then transferred to the Simscape model to simulate movement on the designed platform.

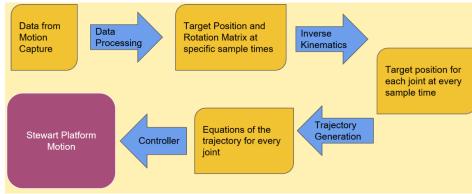


Fig. 8. Flow diagram for System Modelling and Control

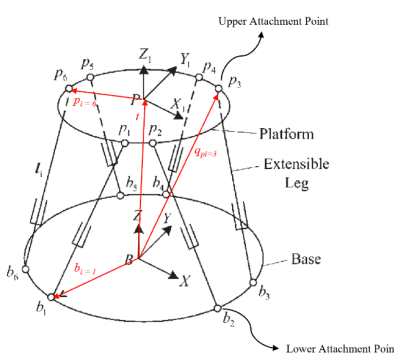


Fig. 9. Schematic diagram of the stewart platform with virtual legs.

1) *Kinematics Analysis:* The inverse position kinematics for the stewart platform was derived as a first step to develop-

oping the controller. The derivation of the inverse position kinematics happens in two steps:

a) *Platform Position to Virtual Leg Length:* In the first step, the position and orientation of the platform is converted into a virtual leg length. A virtual leg is defined as the distance between any lower attachment point to its corresponding upper attachment point. The following vector equation is used to perform this transformation [1]:

$$l_i = (t + R_{p_i}) - b_i$$

Where  $l_i$  is the vector representing the length of the  $i^{\text{th}}$  leg,  $t$  is the distance between the base frame and the platform frame,  $R$  is the Rotation matrix from the base frame to the platform frame,  $b_i$  is the vector representing the position of the base attachment point  $i$  of the  $i^{\text{th}}$  leg with respect to the base frame and  $p_i$  is the vector representing the position of the platform attachment point  $i$  of the  $i^{\text{th}}$  leg with respect to the platform frame.

$t$  can also be thought of as the target position of the platform with respect to the base frame and  $R$  can be thought of as the target rotation of the platform with respect to the base frame

The numerical length of the leg can be found by taking the  $L_2$  norm of the  $l_i$  vector:  $l_i = \|l_i\|$ . Therefore, the unit vector representing the leg can be represented as  $\mathbf{n} = \frac{l_i}{l_i}$

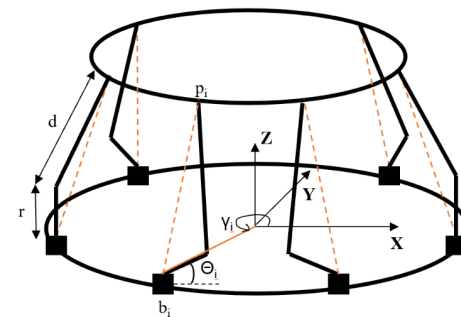


Fig. 10. Schematic diagram of a Stewart platform with rotary actuators

b) *Linear Actuator Position to Rotary Actuator Position:* The relationship between the leg length and motor angle is obtained from Szufnarowski (2013) [10] and is as follows:

Let

$$a_i = 2r(z_{p_i} - z_i)$$

$$b_i = 2r[\sin(\gamma_i)(x_{p_i} - x_i) - \cos(\gamma_i)(y_{p_i} - y_i)]$$

$$c_i = |l_i| - d^2 + r^2$$

Then, the angular position  $\theta_i$  of the  $i^{\text{th}}$  motor can be defined as:

$$\theta_i = \arcsin\left(\frac{c_i(-1)^i}{\sqrt{a_i^2 + b_i^2}}\right) - \arctan\left(\frac{b_i}{a_i}\right)$$

Where,  $r$  is the distance of the servo horn from the centre of the servo to the first attachment point,  $d$  is the distance

from the first attachment point to the platform attachment point  $x_{pi}, y_{pi}$ , and  $z_{pi}$  are the x,y and z direction positions respectively of the  $i^{\text{th}}$  attachment point of the platform with respect to the base frame.  $x_i, y_i$ , and  $z_i$  are the x,y and z direction positions respectively of the  $i^{\text{th}}$  attachment point of the base with respect to the base frame  $\gamma_i$  is the angular position of the  $i^{\text{th}}$  attachment point of the base taking x axis of the base frame as the reference.

In order to find the angular velocity from the rate of change of leg length, we simply differentiate the above theta values with respect to time.

**2) Trajectory Planning:** The purpose of the trajectory planner is to obtain smoother motion of the platform. By interpolating the data points for each joint angle at specified time points and applying constraints, the platform produces more continuous motion. The trajectory planner consists of a set of data points divided into multiple segments over a period of time. The derived joint angles from the inverse kinematics model are taken as the input. The time intervals are set as desired. Depending on the length of the data, the number of time points is calculated. A series of time instances is produced for all segments of the trajectory. The following third-order polynomial equation is used to express the joint trajectory of each segment in terms of t and smoothly interpolate the data.

$$\beta(T_j + \delta t) = a_j 0 + a_j 1t + a_j 2t^2 + a_j 3t^3$$

Where,  $\beta(T_j + \delta t)$  is the equation that defines the joint trajectory,  $t$  is the simulation time, and the  $a$  terms in the equation represent the coefficients of the cubic polynomial.

The following constraints were specified for the planner. The initial and final velocity of the platform is zero. Also, no abrupt changes should be experienced in velocity. Hence, the initial velocity of each segment is made to be equal to the final velocity of the previous segment. By iterating this, the position equations are derived for each segment from joint 1 to joint 6 of the platform.

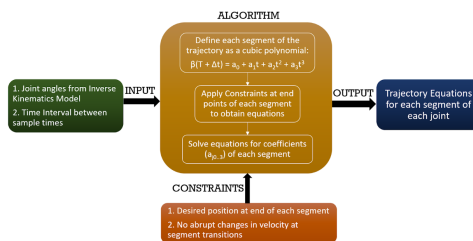


Fig. 11. Flow diagram representation of the Trajectory Planner algorithm

**3) PID Controller:** The control loop model represents a position controller for the actuator of each leg of the Stewart Platform. The approach for solving the control problem of the Stewart Platform was by implementing a PID controller to tune the position and velocity error of the system. The PID controller reduces the difference between the desired and actual positions and velocities of each leg of the Stewart Platform. The PID controller is implemented using Simulink

and the input to the controller are the joint angles that are obtained from the trajectory planner. The plant model implemented in Simulink represents a modified version of a general servo motor. The Kp, Ki, and Kd values of the PID controller have been tuned manually. With the tuned gain values for the data input, it was found that proportional and derivative gain produce ideal results when the integral gain is kept minimal or eliminated. To that effect, the integral gain was eliminated and the PD controller was then implemented in Simscape to merge the control model with the simulated mechanical model of the platform.

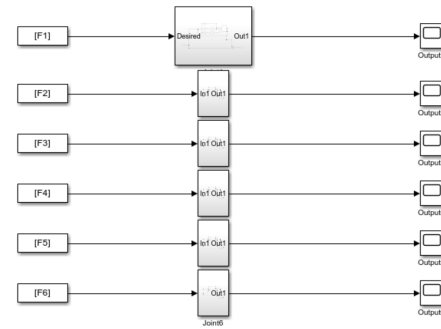


Fig. 12. Simulink model which feeds each joint angle to a PID controller

The PID controller for each of the motor is below with a minimal Integral gain value.

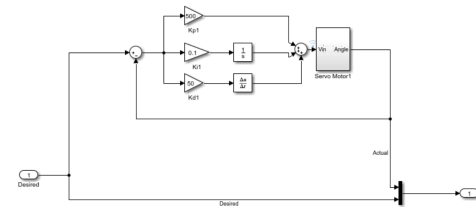


Fig. 13. Simulink model which feeds each joint angle to a PID position and velocity controller

The Controller below is the final version for velocity and position control of one joint:

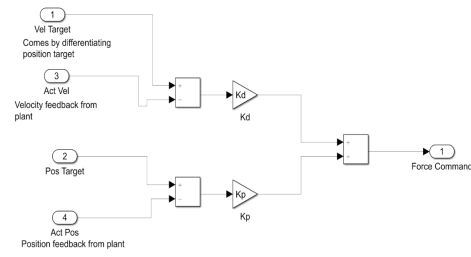


Fig. 14. Full force controller

#### D. Simulation

On completion of the design of our platform, we tried to perform the simulation on Gazebo. We imported the model successfully and found a method to connect our controller in simulink with our model in Gazebo. However, upon running the simulation, a large amount of noise was found in the position and velocity feedback of the joints. In addition to this, we found that Gazebo was solving the simulation in discrete time. These 2 effects together caused our simulation to work in an abnormal fashion. As a result, it was decided that Simscape Multibody would be used for the simulation.

In Simscape Multibody, all the CAD files were imported as STEP files, the rigid transformations between them were defined and the joints between the links were also defined. The revolute joints of the servo motors were defined as torque controlled joints.

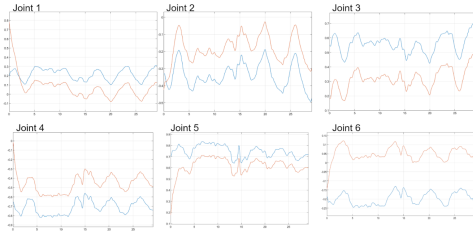


Fig. 15. Visualization of the Stewart Platform in Simscape Multibody. (The servo motors were not rendered in the visualization in order to reduce computation time.)

The output from the trajectory planner is in the form of position equations for each segment of the trajectory for each joint. In order to use these equations to provide input to the Simscape model, a MATLAB function block was used. The MATLAB function associated with this block, takes the simulation time, identifies the appropriate trajectory segment corresponding to the simulation time and uses the corresponding trajectory equation to find the target position. A similar function was written to obtain the target velocities. Here, the trajectory equation is differentiated to obtain the target velocity.

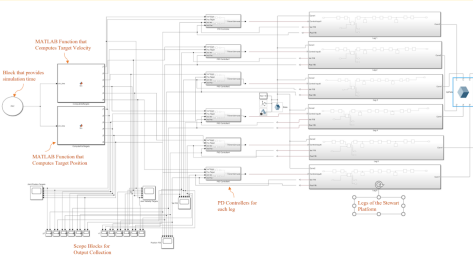


Fig. 16. Complete Simscape Multibody Circuit

### III. RESULTS AND DISCUSSION

#### A. Design Fabrication

The final design of the platform was 3D printed using PLA on Ultimaker-3 and Tazbot printers. To keep the platform light

and sturdy at the same time, the infill density was set at 40 percent.



Fig. 17. 3D printed stewart platform

#### B. Data Processing

The free breathing motion data was used to obtain xyz position data for the platform simulation. After processing and trimming the data as needed, 480 points were obtained for a sampling time of 0.25s. The following graph shows the plotted xyz points for the data.

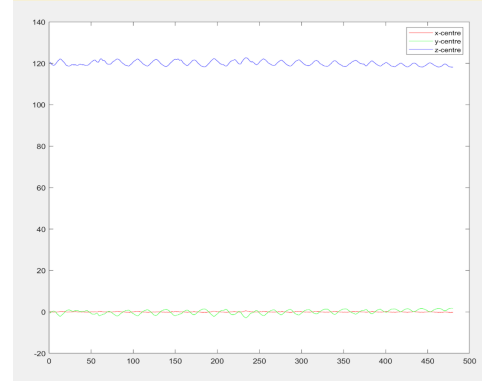


Fig. 18. XYZ data points extracted from breathing motion data. Time(s) vs Angles (rad)

#### C. Trajectory Generation

Given the processed data set, the trajectory was generated for each joint with 479 segments for a period of 120 seconds. The following graph shows the six joint trajectories:

#### D. Joint Position Output

The following graphs represent the motion of each of the 6 joints as compared to the target position. Figure 19 plots the actual and desired positions from the given data points. The tuned K<sub>p</sub>, K<sub>i</sub>, and K<sub>d</sub> values were 500, 0.1, and 50 respectively. There was unavoidable overshoot in the response which may be due to the way the system was modelled.

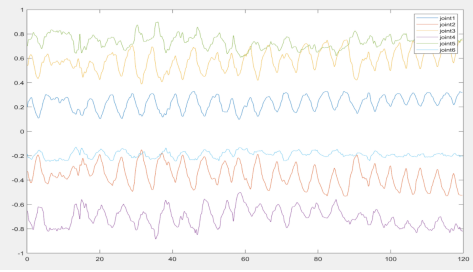


Fig. 19. Joint trajectories for free breathing motion data. Time(s) vs Angles (rad)

Fig 21 shows the actual joint motion when following the given trajectory of free breathing motion data. The errors in the position output are limited and can be further reduced by additional tuning of the Kp and Kd values. Using algorithms such as Ziegler-Nichols for automated PID tuning would show further improved results.

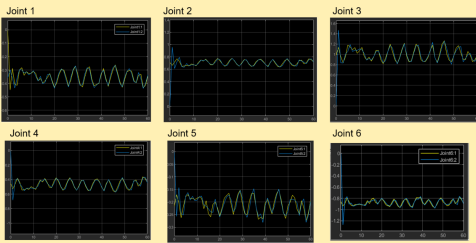


Fig. 20. Results of pid tuning for actual joint position (blue) as compared to desired joint position (yellow)

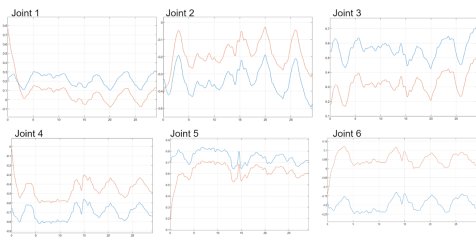


Fig. 21. Actual joint motion (orange) following the given trajectory (blue)

#### E. Joint Velocity Output

The following 6 graphs represent the velocity of each of the 6 joints as compared to the target velocity. The graphs show that the actual joint velocities are almost identical to the target joint velocities.

#### IV. CONCLUSION

In conclusion, this project met its goal of designing, simulating, and building a stewart platform. A modified design was developed for better motion and increased flexibility within the specified workspace constraints. The system model was developed with inverse kinematics, trajectory planning and P-D tuning. The simulation displayed the performance of the

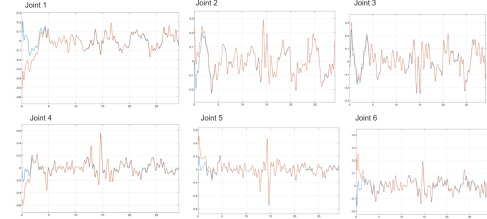


Fig. 22. Actual joint motion (orange) following the given trajectory (blue)

platform. The fabricated model of the stewart platform worked as expected. Further modifications could be made to improve accuracy with automated tuning methods, position and velocity sensors for feedback and higher precision motors.

#### REFERENCES

- [1] H B Guo and H R Li. "Dynamic analysis and simulation of a six degree of freedom Stewart platform manipulator". In: *Proceedings of the Institution of Mechanical Engineers, Part C: Journal of Mechanical Engineering Science* 220.1 (2006), pp. 61–72. DOI: 10.1243/095440605X32075. eprint: <https://doi.org/10.1243/095440605X32075>. URL: <https://doi.org/10.1243/095440605X32075>.
- [2] Daniel T. Kettler et al. "An active motion compensation instrument for beating heart mitral valve surgery". In: *IEEE International Conference on Intelligent Robots and Systems* October (2007), pp. 1290–1295. DOI: 10.1109/IROS.2007.4399543.
- [3] Roger Kneebone. "Simulation in surgical training: Educational issues and practical implications". In: *Medical Education* 37.3 (2003), pp. 267–277. ISSN: 03080110. DOI: 10.1046/j.1365-2923.2003.01440.x.
- [4] Yoshihiko Nakamura, Kosukke Kishi, and Hiro Kawakami. "Heartbeat Synchronization for Robotic Cardiac Surgery". In: *IEEE International Conference on Robotics & Automation* 53.9 (2001), pp. 1689–1699. ISSN: 1098-6596. DOI: 10.1017/CBO9781107415324.004. arXiv: arXiv:1011.1669v3.
- [5] Vanessa Palter and Teodor Grantcharov. "Simulation in Surgical Education". In: 182.11 (2010), pp. 1191–1196. DOI: 10.1503/cmaj.091743.
- [6] Vatsal Patel et al. "SPRK: A low-cost stewart platform for motion study in surgical robotics". In: *2018 International Symposium on Medical Robotics, ISMR 2018* 2018-January. Figure 2 (2018), pp. 1–6. DOI: 10.1109/ISMR.2018.8333300.
- [7] Cameron N. Riviere, Jacques Gangloff, and Michel De Mathelin. "Robotic compensation of biological motion to enhance surgical accuracy". In: *Proceedings of the IEEE* 94.9 (2006), pp. 1705–1715. ISSN: 00189219. DOI: 10.1109/JPROC.2006.880722.
- [8] A. Schweikard et al. "Robotic motion compensation for respiratory movement during radiosurgery". In: *Computer Aided Surgery* 5.4 (2000), pp. 263–277. ISSN: 10929088. DOI: 10.1002/1097-0150(2000)5.

- [9] Ghufraan Shafiq and Kalyana Chakravarthy Veluvolu. "Corrigendum: Multimodal chest surface motion data for respiratory and cardiovascular monitoring applications". In: *Scientific data* 4 (2017), p. 170099. ISSN: 20524463. DOI: 10.1038/sdata.2017.99.
- [10] Filip Szufnarowski. *Stewart platform with fixed rotary actuators: a low cost design study*. Tech. rep.
- [11] Jürgen Wilbert et al. "Tumor tracking and motion compensation with an adaptive tumor tracking system (ATTS): System description and prototype testing". In: *Medical Physics* 35.9 (2008), pp. 3911–3921. ISSN: 00942405. DOI: 10.1118/1.2964090.
- [12] Shelten G. Yuen et al. "Robotic motion compensation for beating heart intracardiac surgery". In: *International Journal of Robotics Research* 28.10 (2009), pp. 1355–1372. ISSN: 02783649. DOI: 10 . 1177 / 0278364909104065.